

Effect of Silver Nanoparticles on the Electron Transfer Reactivity and the Catalytic Activity of Myoglobin

Xin Gan, Tao Liu, Jun Zhong, Xinjian Liu, and Genxi Li*^[a]

Silver nanoparticles (11 ± 1.5 nm) could greatly enhance the electron-transfer reactivity of myoglobin (Mb) and its catalytic ability toward hydrogen peroxide (H_2O_2). Direct fast electron transfer between Mb and a pyrolytic graphite (PG) electrode was achieved, and a pair of well-defined, quasireversible redox peaks was obtained. The cathodic and anodic peaks were located at -329 and -281 mV, respectively. Meanwhile, the catalytic ability of the protein toward the reduction of H_2O_2 was also studied, and a H_2O_2 biosensor was subsequently fabricated. Its detection limit

was 1.0×10^{-6} M with a sensitivity of $0.0205 \mu A$ per μM of H_2O_2 . The apparent Michaelis–Menten constant was calculated to be $1303 \mu M$. Flocculation assay showed that the protein maintained plasmon layers surrounding the surface of silver nanoparticles and avoided silver-nanoparticle aggregation. On the other hand, UV-visible spectroscopy studies revealed that silver nanoparticles could induce a small change of the heme-group environment of the protein; this contributed to the enhancement of the electron-transfer reactivity and the catalytic activity.

Introduction

Nanoparticles (NPs) have emerged as a new kind of inspective material and have quickly come to play important roles in different areas. In an extraordinarily short time, NPs, such as Au, CdSe, TiO_2 , and carbon nanotubes, have been widely exploited in the study of electronics (quantum-dots), catalysis,^[1] biomodeling,^[2] biolabeling,^[3] sensing,^[4] surface-enhanced Raman scattering (SERS),^[5] photonics,^[6] and optoelectronics^[7] due to their special characters induced by the size of the particles.

Due to its serviceability, novelty, and variety, nanoscale science has greatly intersected biological study and has recently attracted much attention due to its application in many fields in biology. For example, Alivisatos and Nie et al. used functionalized nano-CdS particles as a fluorescence probe for the determination of proteins.^[3a,b,8] Bergemann et al. developed a group of magnetic nanoparticles in the application of cell and drug targeting, gene-transfection studies, and DNA extraction.^[9] Meanwhile, lots of findings with gold NPs have been obtained,^[10] such as enhancing DNA immobilization and its specific sequence-hybridization detection^[10a] and supporting the nanowiring of redox enzymes.^[10b] The direct electrochemistry response of hemoglobin has been obtained at gold NP–cysteamine-modified gold electrode.^[10e] Moreover, the detection limit in surface plasmon resonance (SPR)-based real-time biospecific-interaction analysis has also been enhanced by gold NPs.^[10f,g]

Although more and more nanomaterials are available, only a few kinds of NP have been used in biological studies. Silver NPs, which are easy to synthesize, have attracted our attention due to their quantum characteristics of small granule diameter and large specific surface area as well as their ability to quickly transfer photoinduced electrons at the surfaces of colloidal particles.^[11]

As an oxygen-transport protein found in cardiac and red skeletal muscles, myoglobin (Mb), which has a molecular

weight (M_w) of 17000 and a single electroactive iron heme as a prosthetic group,^[12] is often used as a model to study the structure and function of heme proteins. However, since the heme group in Mb is buried deeply in the peptide chains, the electron transfer (eT) process between the protein and electrode is much more inhibited than other in heme proteins, such as hemoglobin and cytochrome c; thus Mb has poorer eT kinetics and redox properties.^[13] So far, some electron shuttles have been employed to obtain good electrochemical communication between Mb and electrodes. Now we claim that NPs might be a competent material for making such shuttles. Experimental results have revealed that a fast eT rate of Mb can be obtained with the help of silver NPs, and a pair of well-defined redox peaks can be observed at a pyrolytic graphite (PG) electrode. The catalytic ability and sensitivity of Mb have also been improved by the silver NPs.

Results and Discussion

The redox reactivity of Mb at a bare PG electrode surface is too small to measure. But, with the effect of silver NPs, the protein can make a direct fast eT with the substrate electrode. As is shown in Figure 1 (solid curve), when a Mb–silver NP-modified ($V_{Mb}/V_{colloid}$ 7:1) electrode is inserted in 0.1 M phosphate buffer solution (PBS) at pH 6.0, a pair of well-defined, quasireversible redox peaks can be observed. In contrast, there is no peak observed at a bare PG electrode (Figure 1, dotted

[a] X. Gan, T. Liu, J. Zhong, X. Liu, Prof. Dr. G. Li
Department of Biochemistry and
National Key Laboratory of Pharmaceutical Biotechnology
Nanjing University
Nanjing 210093 (P. R. China)
Fax: (+86) 25-835-92510
E-mail: genxili@nju.edu.cn

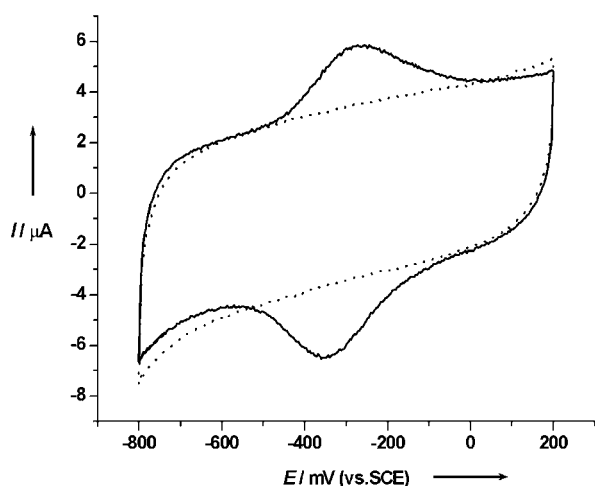


Figure 1. Cyclic voltammograms of 0.1 M PBS at pH 6.0 obtained at the bare PG (dotted curve) and Mb-silver NPs/PG electrode (solid curve) with $V_{\text{Mb}}/V_{\text{colloid}}$ 7:1. Scan rate: 200 mV s^{-1} .

curve). No peak exists in this potential range with a PG electrode modified just by silver NPs. Therefore, these two peaks arise from the redox reactions of Mb immobilized at the electrode surface. The cathodic and anodic peak potentials are located at -329 and -281 mV, respectively. The formal potential (E^0) is calculated to be -305 mV, which is similar to a previous report.^[14] The peak separation is 48 mV; this indicates a fast, quasireversible, one-electron, heterogeneous eT process.

The pH value of the background solution plays an important role in the electrochemical reactions of Mb modified on the electrode surface. Experimental results reveal that the formal potential (E^0) of Mb will shift negatively with increasing pH value. Moreover, the relation between E^0 and pH value is linearly proportional in the range from 4.0 to 10.0 (Figure 2), with a linear regression equation of $y = -5.6018 - 49.1804x$, $r = 0.998$. The slope of the plot is -49.1804 mV per one point change in pH; this might imply that the redox reaction is a coupling of a single electron with a single proton.^[15]

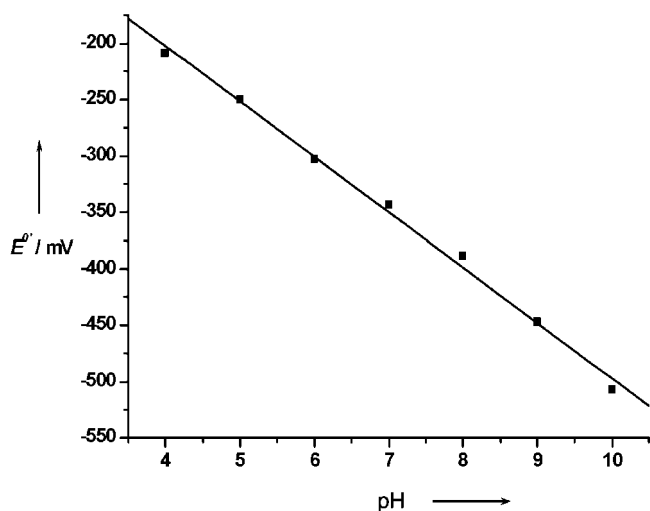


Figure 2. Effect of pH on the formal potential (E^0) of Mb.

Figure 3 shows the relationship between the peaks currents (I) of Mb and the scan rate (v). Both the cathodic and anodic peak currents are linearly proportional to the scan rate; this is the characteristic of thin-layer electrochemical behavior. (Linear regression equations: $y = 0.1746 + 0.00521x$, $r = 0.999$; $y =$

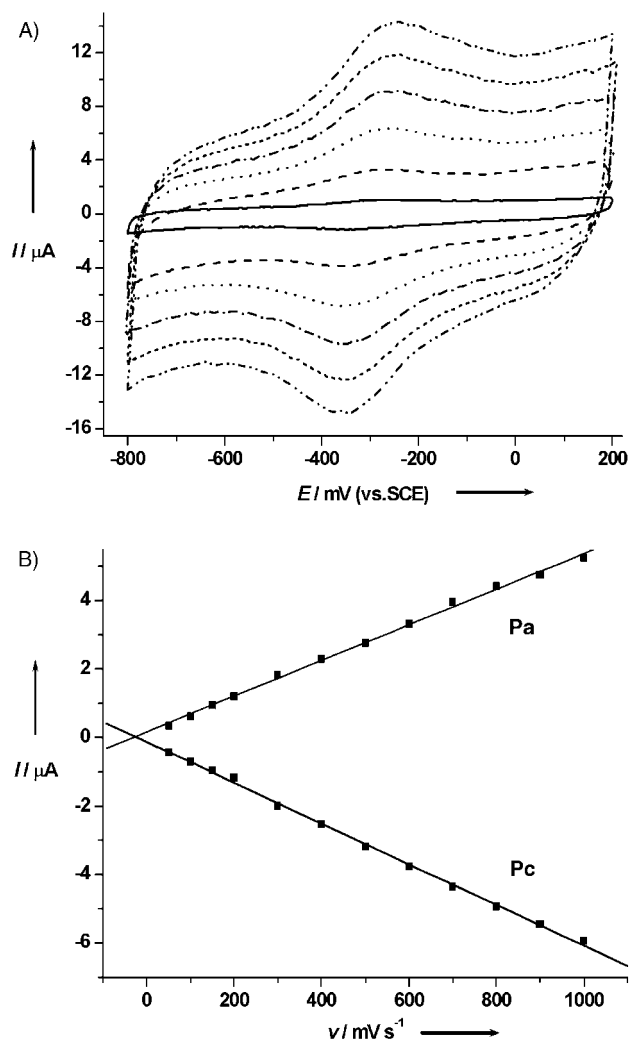


Figure 3. A) Cyclic voltammograms of 0.1 M PBS obtained at the Mb-silver NPs/PG electrode with $V_{\text{Mb}}/V_{\text{colloid}}$ 7:1 at scan rates of 50, 200, 400, 600, 800, 1000 mV s^{-1} (from inner to outer). B) Relationship between scan rate (v) and the cathodic (Pc) and anodic (Pa) peak current (I) of Mb.

$-0.1251 - 0.00594x$, $r = 0.999$.) The slopes obtained by linear regression of both $\log I_{\text{Pa}}$ and $\log I_{\text{Pc}}$ versus $\log v$ are 0.916 and 0.914, respectively; this suggests that most ferrous Mb on the electrode will convert to met-Mb on a positive direction CV scan and vice versa. Meanwhile, Figure 4 shows that the cathodic peak potential E_p is linear to $\ln(v)$, with a linear regression equation of $y = -0.3689 - 0.03905x$, $r = 0.999$ in the potential scan range from 300 to 1000 mV s^{-1} . According to Laviron's Equation:^[16]

$$E_p = E^0 + \frac{RT}{\alpha nF} - \frac{RT}{\alpha nF \times \ln(v)} \quad (1)$$

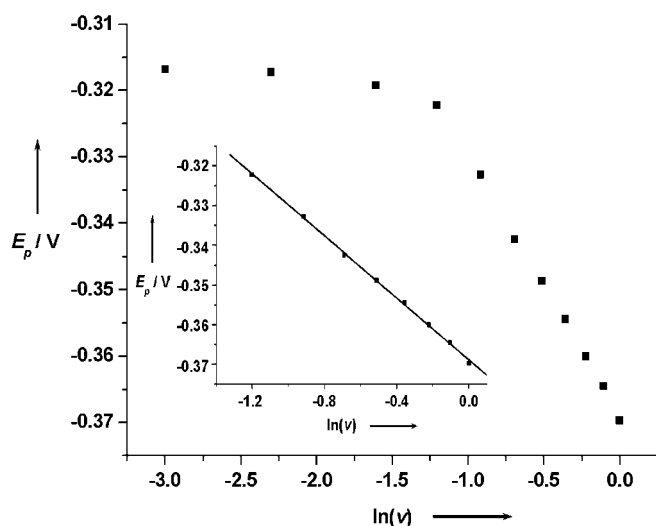


Figure 4. The cathodic peak potential (E_p) versus $\ln(v)$ and its line fitting at scan rates from 300–1000 mVs^{-1} (inset).

Here α is the charge transfer coefficient and n is the number of electrons, $\alpha \times n$ is calculated as 0.65. Given $0.3 < \alpha < 0.7$ in general, we conclude that $n=1$ and $\alpha=0.65$. So, the redox reaction of Mb is a single eT process.

The eT rate of Mb at silver NPs co-modified electrodes has also been calculated. Given α in Equation (1) being 0.65, K_s is calculated out to be 12.22 s^{-1} ,^[17] which is much higher than in previous reports, for instance, 0.93 s^{-1} gained at the DL-homocysteine self-assembled gold electrode.^[18] So silver NPs play a very important role in the eT reaction of Mb. Silver NPs might not only help the protein structure to keep its biological activity, but also act as a wire between the protein and electrode.

Silver NPs will also affect the amount of the protein adsorbed. The surface adsorption amount (Γ) of Mb can be obtained according to Equation (2):

$$\Gamma = Q/nFA \quad (2)$$

Here Q , n , and A stand for the reduction charge, the number of transferred electrons, and the effective area of the electrode surface, respectively. The relationship between the protein coverage and the proportion of silver NPs and Mb is shown in Table 1. The results clearly show that the proportion of protein

Table 1. Relationship between protein coverage (Γ [mol cm^{-2}]) and $V_{\text{Mb}}/V_{\text{col}}$ proportion.

$V_{\text{Mb}}/V_{\text{colloid}}$	2:1	4:1	5:1	6:1	7:1	8:1	10:1
Γ ($\times 10^{-10}$)	1.418	1.699	1.865	2.398	3.026	2.614	1.810

and silver NPs will affect the protein coverage at the electrode surface. When the proportion of $V_{\text{Mb}}/V_{\text{colloid}}$ is 7:1, the adsorbed amount of the protein is highest, so best electrochemical response may be obtained. We thus selected this proportion for this work.

When the proportion of $V_{\text{Mb}}/V_{\text{colloid}}$ is 7:1, the surface coverage of Mb is $3.026 \times 10^{-10} \text{ mol cm}^{-2}$, which is much larger than that of a previous report.^[19] So silver NPs can greatly increase the amount of the protein at the electrode. This might be one of the reasons that Mb exhibits good redox activity in this work.

Therefore, although Mb exhibits a rather slow rate of heterogeneous eT at conventional electrodes,^[20] because of the deep burying of the electroactive prosthetic groups, adsorptive denaturation of proteins onto electrodes and unfavorable orientations at electrodes, with the help of silver NPs a part of redox peaks of Mb can be observed. Silver NPs might have decreased the electric resistance between protein and electrode by relaxing the hydrophobic pocket of Mb and changing the environment of the porphyrin ring; this may be supported by the following studies.

UV-visible absorption spectra can give information about the environment surrounding the heme group of Mb. The Soret band of Mb is located at 409.0 nm,^[22] which is an intrinsic heme-group property. Its position and shape can reflect the identity of the axial ligand as well as the heme group environment.^[21] Previous studies have revealed that the Soret absorption band of Mb will decrease or even disappear if the axial ligand has been changed.^[22] Figure 5 shows the UV-visible ab-

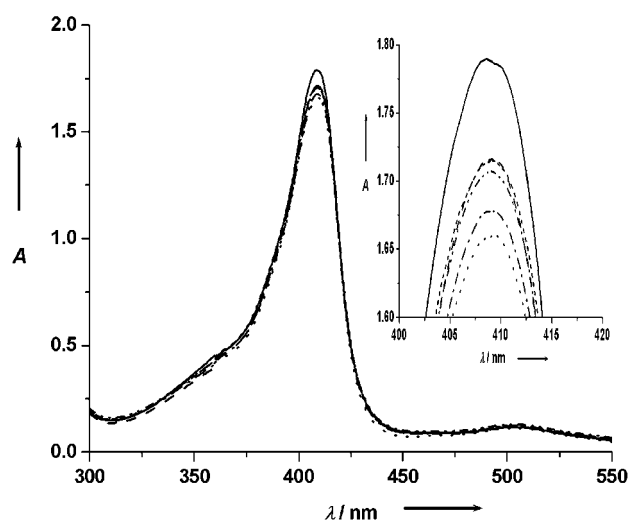


Figure 5. UV/vis absorption spectra of Mb in solution (the solid curve) and bioconjugates of Mb and silver NPs with $V_{\text{Mb}}/V_{\text{colloid}}$ proportions of 10:1, 8:1, 6:1, 4:1, and 2:1 (from outer to inner). Mb concentration: 0.3 mg mL^{-1} . Inset: enlarged view of the absorbance peaks.

sorption of a series of different ratios of Mb and silver NPs. With an increasing ratio of silver NPs, the Soret bands shift from 409.0 nm to 409.3 nm; these values are very close to the peak location of pure Mb, but the spectral absorbance of the Soret band decreases gradually with the increasing proportion of silver NPs. This result indicates that the heme environment can gently change the Mb conformation, but not to the extent of destroying it. In the natural state, the redox center of the porphyrin ring is mostly located deeply inside the hydrophobic

pocket near the surface of the molecule.^[20a] After silver NPs have been dissolved in the solution of Mb, they may interact with the Lys fragments outside the hydrophobic pocket of the heme group, inducing the tethered pocket to relax and the inner porphyrin ring to become dome-shaped close to the surface of hydrophobic pocket. This rearrangement influences Mb's UV-visible absorption spectrum, and results in a good electrochemical response of Mb.

The interaction between the protein and silver NPs has also been assessed by flocculation assay. It is been known that just the addition of electrolytes into a silver colloid will cause silver NPs to flocculate.^[5a] The aggregation can be conveniently monitored photometrically by the decrease in the plasmon absorption band of silver NPs at about 422.5 nm. Figure 6 shows

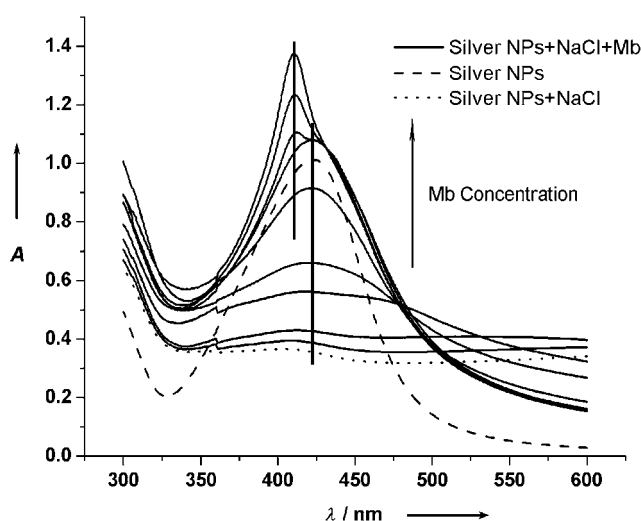


Figure 6. Flocculation assay of silver NPs, silver NPs with NaCl, and the NPs with NaCl and Mb at different concentrations (0.20, 0.16, 0.13, 0.1, 5.0×10^{-2} , 1.0×10^{-2} , 5.0×10^{-3} , 1.0×10^{-3} , and 5.0×10^{-4} mg mL^{-1} from top to bottom at the peak). Silver NPs concentration: 1.20×10^{-9} M.

the flocculation assay of silver NPs, silver NPs with NaCl, and the NPs with NaCl and Mb at different concentrations. It shows that the original absorption band of silver NPs at 422.5 nm decreases sharply after electrolytes are added to the silver colloid. However, as more Mb is added to the solution, the aggregative extent of the silver NPs decreases. Therefore, the plasmon resonance layers of silver NPs, which are supposed to be destroyed by electrolytes, can remain because of the new special links formed between the added protein and the NPs. Mb has been bound to the silver NPs, blocking their active sites to the binding of electrolytes; thus, the electrolytes have a reduced effect on the aggregation of silver NPs. Accordingly, the absorption band of silver NPs regresses gradually, and finally maintains its absorption as normal at the Mb concentration of 0.1 mg mL^{-1} . Since the concentration of Mb used in our study is high above this concentration limit, no aggregation should happen in our system.

Thus, we consider that there may be several possible factors benefiting the fast eT between protein and electrode. Firstly,

the silver NPs system itself can transfer an electron, and its conjugating with Mb may create a fast electron-conducting tunnel, which will greatly facilitate the eT between protein and electrode. Secondly, just as the measurements of UV-visible spectra denoted, silver NPs partially change the inner micro-environment of the heme group; this results in the opening of the electroactive center and makes it closed to Mb surface. Silver NPs may have jointed each other to provide a faster eT tunnel through protein and electrode.

The main function of Mb in mammals is to transport oxygen. However, it also has potential peroxidase activity to catalyze the reduction of small molecules, such as H_2O_2 ,^[23] NO ,^[24] and so on. Figure 7 shows the cyclic voltammogram of

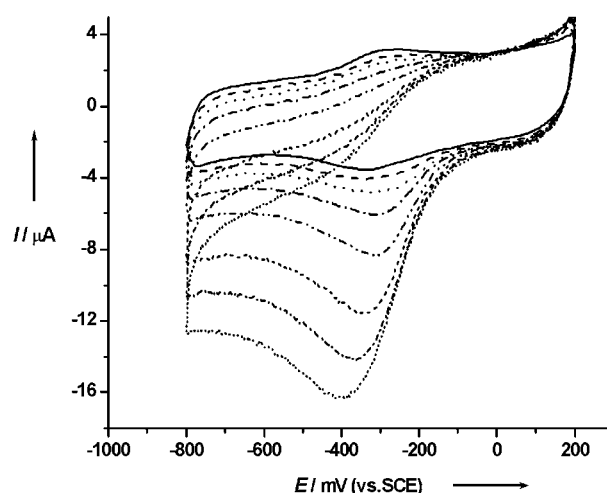
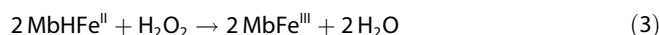


Figure 7. Cyclic voltammograms obtained at the Mb-silver NPs/PGE electrode with $V_{\text{Mb}}/V_{\text{colloid}}$ 7:1 for 0.1 M PBS at pH 6.0 with H_2O_2 concentrations of 0 (solid curve), 3×10^{-5} , 5×10^{-5} , 1×10^{-4} , 2×10^{-4} , 4×10^{-4} , 5×10^{-4} , 6×10^{-4} M (from top to bottom).

the modified electrode in 0.1 M PBS at pH 6.0 containing different concentrations of H_2O_2 . A new obvious reduction peak can be observed, and this catalytic peak increases with increased H_2O_2 . With catalytic peak current increasing, the anodic peak of Mb decreases and even disappears; this may be attributed to the oxidation of Fe^{II} to Fe^{III} by H_2O_2 [Equation (3)]:



Comparably, no corresponding electrochemical signal is observed with either a bare PG electrode or a PG electrode modified with just silver NPs under the same conditions. So the catalytic peak must come from the enzymatic catalytic reaction of Mb toward H_2O_2 .

A linear dependence of the reduction peak current and the concentration of H_2O_2 is found in the range of 3.0×10^{-6} ~ 7.0×10^{-4} M (Figure 8). The linear-regression equation is $y = 3.8239 + 0.0205x$, $r = 0.998$. Its detection limit is 1.0×10^{-6} M with a sensitivity of $0.0205 \mu\text{A}$ per μM of H_2O_2 . When the concentration of H_2O_2 is higher than 7.0×10^{-4} M, a platform emerges in the catalytic peak current; this accords with the Michaelis-

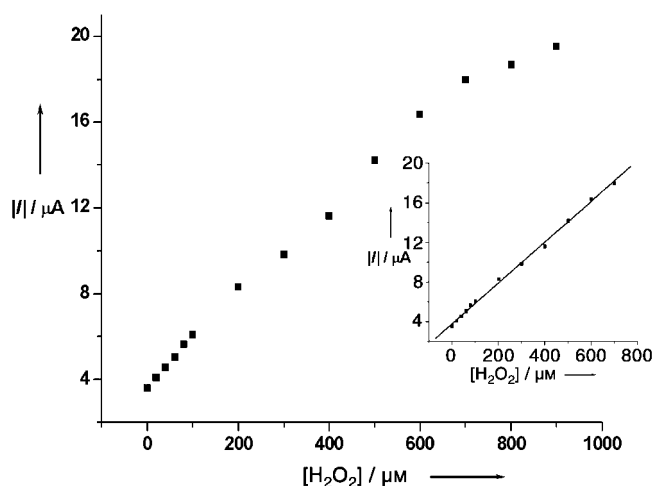


Figure 8. Relationship between H_2O_2 concentration and the cathodic peak current of Mb. Inset: its linear fitting program with $[\text{H}_2\text{O}_2]$ from 3.0×10^{-6} – 7.0×10^{-4} M.

Menten model. The apparent Michaelis–Menten constant (K_m^{app}) is $1303 \mu\text{M}$ as calculated by the Lineweaver–Burk equation:^[25]

$$\frac{1}{I_{\text{ss}}} = \frac{1}{I_{\text{max}}} + \frac{K_m^{\text{app}}}{I_{\text{max}} \times c} \quad (4)$$

Here I_{ss} , I_{max} and c stand for steady current, maximum current, and H_2O_2 concentration, respectively. It is well known that a smaller K_m^{app} represents a higher catalytic ability. Since this is much smaller here than the $2280 \mu\text{M}$ obtained with a cytochrome *c*-Au-carbon paste electrode (CPE)^[26] or the $3690 \mu\text{M}$ of a horseradish peroxidase–Au–CPE,^[10c] it is indicated that the affinity of Mb and H_2O_2 is much higher than that obtained from other films or NPs.

From the above results, it can be deduced that silver NPs have changed the environment of heme group, and may make the redox center of Mb active. Moreover, silver NPs possibly act like a network of eT tunnels, which promote the sensitivity of the protein to its catalytic substrates. It could be used as a potential sensitive biosensor in the trace determination of H_2O_2 .

Conclusion

The eT reactivity and catalytic ability of Mb can be greatly enhanced with the help of silver nanoparticles. A good electrochemical response from Mb is obtained at the PG electrode modified by Mb/silver NPs. The protein maintains the plasmon layers of the silver NPs and prevents their aggregation. Meanwhile, silver NPs might greatly influence the environment of the electroactive center of Mb. They also act as eT tunnels to greatly facilitate electron transfer between the protein and electrode. This modified electrode could also be used as an alternative hydrogen peroxide biosensor.

Experimental Section

Chemicals and apparatus: Horse heart Mb was obtained from Sigma and used without any purification. AgNO_3 was purchased from the Shanghai No.1 Reagent Factory (China). Other chemicals were all of analytical grade. All solutions were prepared with double-distilled water, which was purified with a Milli-Q purification system (Branstead, USA) to a specific resistance of $> 16 \text{ M}\Omega \text{ cm}^{-1}$ and stored in the refrigerator at 4°C .

Electrochemical experiments were carried out with a VMP Potentiostat (Perkin–Elmer, USA) and a three-electrode system. A one-compartment glass cell with a modified PG working electrode, a saturated calomel reference electrode (SCE), and a platinum-wire auxiliary electrode were used for the measurements, with a working volume of 10 mL. All the following potentials reported in this work are against the SCE.

The size of silver colloid was measured with a JEX-200CX transmission electron microscope (JEOL, Japan). UV/vis absorption spectroscopy and flocculation assays were performed on a Model UV-2201 spectrophotometer (Shimadzu, Japan).

Silver NP preparation: Silver NPs were prepared according to the literature.^[27] Tannic acid (1.0 mL, 5.88 mM) was added to a vigorously stirring aqueous solution of AgNO_3 (100 mL, 2.0 mM), then an aqueous solution of K_2CO_3 (0.2 mL, 1%) was added. All the glassware was firstly washed with freshly prepared HNO_3/HCl (1:3, v/v), then rinsed thoroughly with double-distilled water and dried in air. The concentration of silver NP solution was $3.59 \times 10^{-9} \text{ M}$, and the solution was stored at 4°C in a refrigerator. TEM measurements indicated that the average silver nanoparticle size was $11 \pm 1.5 \text{ nm}$ (100 particles sampled).

Preparation of modified electrodes: The substrate PG electrode was prepared by putting a PG rod into a glass tube and fixing it by epoxy resin. Electrical contact was made by adhering a copper wire to the rod with the help of Wood alloy.

The PG electrode was firstly polished on rough and fine sand papers. Then its surface was polished to mirror smoothness with an alumina (particle size of about $0.05 \mu\text{m}$)/water slurry on silk. Eventually, the electrode was thoroughly washed by ultrasonication in both double-distilled water and ethanol for about 5 min.

A series of integral proportions of Mb solutions (10 mg mL^{-1}) and silver NPs were spread evenly onto the surfaces of the PG disk electrodes. The electrode surfaces were covered with Eppendorf tubes during the first two hours so as to prepare uniform films. The electrodes were then dried overnight in air. Finally, the modified electrodes were thoroughly rinsed with pure water. They were stored in aqueous solutions of $\text{Na}_2\text{HPO}_4/\text{NaH}_2\text{PO}_4$ (0.1 M) at pH 6.0 and 4°C when they were not in use.

UV-visible absorption spectroscopy measurements: The UV/vis absorption spectra measurements were performed in a Mb (0.3 mg mL^{-1}) solution or in mixed solutions of integral proportions of Mb (0.3 mg mL^{-1}) and silver NPs solutions (Mb maintained 0.3 mg mL^{-1} in the test sample).

Flocculation assay: The bioconjugates of Mb and silver NPs were prepared at a constant silver concentration ($1.20 \times 10^{-9} \text{ M}$) and a series of Mb concentrations. After several minutes' conjugation, the aggregation agent (NaCl, 1 M) was added to each solution.

Electrochemical measurements: The test buffer solution was firstly bubbled thoroughly with high-purity nitrogen for at least 5 min. Then a stream of nitrogen was blown gently across the surface of

the solution in order to keep the solution anaerobic throughout the experiment. Cyclic voltammetry (CV) was carried out in the scan range from 200 to -800 mV. All experiments were carried out at room temperature.

Acknowledgements

We thank the National Natural Science Foundation of China (Grant No. 30070214) and the Chinese Ministry of Education (Grant No. 01087) for financial support.

Keywords: electrochemistry · electrodes · myoglobin · nanoparticles · silver

- [1] a) L. N. Lewis, *Chem. Rev.* **1993**, *93*, 2693–2730; b) M. Haruta, M. Daté, *Appl. Catal. A* **2001**, *222*, 427–437.
- [2] a) R. Mahtab, J. P. Rogers, C. P. Singleton, C. J. Murphy, *J. Am. Chem. Soc.* **1996**, *118*, 7028–7032; b) R. Mahtab, H. H. Harden, C. J. Murphy, *J. Am. Chem. Soc.* **2000**, *122*, 14–17.
- [3] a) M. Bruchez, Jr., M. Moronne, P. Gin, S. Weiss, A. P. Alivisatos, *Science* **1998**, *281*, 2013–2015; b) W. C. W. Chan, S. M. Nie, *Science* **1998**, *281*, 2016–2018; c) S. R. Nicewarner-Peña, R. G. Freeman, B. D. Reiss, L. He, D. J. Peña, I. D. Walton, R. Cromer, C. D. Keating, M. J. Natan, *Science* **2001**, *294*, 137–141.
- [4] A. J. Haes, R. P. Van Duyne, *J. Am. Chem. Soc.* **2002**, *124*, 10596–10604.
- [5] a) C. D. Keating, K. M. Kovaleski, M. J. Natan, *J. Phys. Chem. B* **1998**, *102*, 9404–9413; b) C. D. Keating, K. M. Kovaleski, M. J. Natan, *J. Phys. Chem. B* **1998**, *102*, 9414–9425.
- [6] S. A. Maier, M. L. Brongersma, P. G. Kik, S. Meltzer, A. G. Requicha Ari, H. A. Atwater, *Adv. Mater.* **2001**, *13*, 1501–1505.
- [7] P. V. Kamat, *J. Phys. Chem. B* **2002**, *106*, 7729–7744.
- [8] a) A. P. Alivisatos, *Pure Appl. Chem.* **2000**, *72*, 3–9; b) H. Mattoussi, J. M. Mauro, E. R. Goldman, G. P. Anderson, V. C. Sundar, F. V. Mikulec, M. G. Bawendi, *J. Am. Chem. Soc.* **2000**, *122*, 12142–12150.
- [9] C. Bergemann, D. Müller-Schulte, J. Oster, L. à Brassard, A. S. Lübbe, *J. Magn. Magn. Mater.* **1999**, *194*, 45–52.
- [10] a) S. Park, T. A. Taton, C. A. Mirkin, *Science* **2002**, *295*, 1503–1506; b) Y. Xiao, F. Patolsky, E. Katz, J. F. Hainfeld, I. Willner, *Science* **2003**, *299*, 1877–1881; c) S. Liu, H. Ju, *Anal. Biochem.* **2002**, *307*(1), 110–116; d) Y. Xiao, H. Ju, H. Chen, *Anal. Biochem.* **2000**, *278*, 22–28; e) H. Gu, A. Yu, H. Chen, *J. Electroanal. Chem.* **2001**, *516*, 119–126; f) L. A. Lyon, M. D. Musick, M. J. Natan, *Anal. Chem.* **1998**, *70*, 5177–5183; g) L. He, M. D. Musick, S. R. Nicewarner, F. G. Salinas, S. J. Benkovic, M. J. Natan, C. D. Keating, *J. Am. Chem. Soc.* **2000**, *122*, 9071–9077.
- [11] a) J. Zheng, G. Chumanov, T. M. Cotton, *Chem. Phys. Lett.* **2001**, *349*, 367–370; b) T. Liu, J. Zhong, X. Gan, C. Fan, G. Li, N. Matsuda, *Chem-PhysChem* **2003**, *4*, 1364–1366.
- [12] B. C. King, F. M. Hawkridge, B. M. Hoffman, *J. Am. Chem. Soc.* **1992**, *114*, 10603–10608.
- [13] a) B. C. King, F. M. Hawkridge, *J. Electroanal. Chem. Interfacial Electrochem.* **1987**, *237*, 81–92; b) I. Taniguchi, K. Watanabe, M. Tominaga, F. M. Hawkridge, *J. Electroanal. Chem.* **1992**, *333*, 331–338.
- [14] P. A. Loach in *Handbook of Biochemistry Selected Data for Molecular Biology*, 2nd ed., (Ed.: H. A. Sober), CRC Press, Cleveland, **1970**.
- [15] a) L. Meites, *Polarographic Techniques*, 2nd ed., Wiley, New York, **1965**; b) A. M. Bond, *Modern Polarographic Methods in Analytical Chemistry*, Marcel Dekker, New York, **1980**.
- [16] E. Laviron, *J. Electroanal. Chem. Interfacial Electrochem.* **1979**, *52*, 355–399.
- [17] E. Laviron, *J. Electroanal. Chem. Interfacial Electrochem.* **1979**, *101*, 19–28.
- [18] H. Zhang, N. Li, *Bioelectrochemistry* **2000**, *53*, 97–101.
- [19] L. Wang, N. Hu, *J. Colloid Interface Sci.* **2001**, *236*, 166–172.
- [20] a) E. Stellwagen, *Nature* **1978**, *275*, 73–74; b) F. A. Armstrong, H. Allen, H. A. O. Hill, N. J. Walton, *Q. Rev. Biophys.* **1985**, *18*, 261–322.
- [21] I. B. Bersuker, S. S. Stavrov, *Coord. Chem. Rev.* **1988**, *88*, 1–68.
- [22] a) H. Theorell, A. Ehrenberg, *Acta Chem. Scand.* **1951**, *5*, 823–848; b) A. E. F. Nassar, W. S. Willis, J. F. Rusling, *Anal. Chem.* **1995**, *67*, 2386–2392.
- [23] D. J. Kelman, J. A. DeGray, R. P. Mason, *J. Biol. Chem.* **1994**, *269*, 7458–7463.
- [24] G. Reichenbach, S. Sabatini, R. Palombi, C. A. Palmerini, *Nitric Oxide Biol. Chem.* **2001**, *5*, 395–401.
- [25] R. A. Kamin, G. S. Wilson, *Anal. Chem.* **1980**, *52*, 1198–1205.
- [26] H. Ju, S. Liu, B. Ge, F. Lisdat, F. W. Scheller, *Electroanalysis* **2002**, *14*, 141–147.
- [27] a) K. Chou, C. Ren, *Mater. Chem. Phys.* **2000**, *64*, 241–246; b) M. Si, P. Zhang, *Guangpuxue Yu Guangpu Fenxi (Spectrosc. Spectral Anal.)* **2001**, *21*, 501–502.

Received: March 27, 2004

Early View Article
Published online on November 3, 2004